JOURNAL OF MATERIALS SCIENCE 24 (1989) 173–182

The microhardness of injection moulded polystyrene and polyethylene

B. L. EVANS
J.J. Thomson Physical Laboratory, University of Reading, Whiteknights, Box 220, Reading, Berkshire, UK

Injection moulded plaques of polystyrene and of two types of high density polyethylene have been produced under different moulding conditions. The mean density ϱ of each plaque together with its surface microhardness V_H have been measured. Polystyrene shows only a slight increase in ϱ with increasing mould temperature T_m together with a reduced spread in ϱ and V_H values. In polyethylene, however, ϱ and V_H both increase linearly with T_m, giving a useful V_H against ϱ relation, which is attributed to increased percentage crystallinity.

1. Introduction

In the commercial production of injection mouldings the operating conditions are often chosen so as to produce visually acceptable polymer mouldings of the required dimensions at the maximum possible rate. In practice this means using the lowest possible melt and mould temperatures thereby minimizing the cooling time. This approach, which ignores the effect of processing conditions on microstructure, can result in mouldings which contain an undesirable molecular orientation or residual strain. Such mouldings may subsequently warp, crack, exhibit poor corrosion resistance or fail in service.

In situations where the frozen in strain or microstructure seriously affects the performance of the moulded polymer it is necessary to establish the correct moulding conditions by experiment. If the polymer is transparent then some indication of the frozen in strain distribution can be obtained from the strain induced birefringence patterns observed in the moulded item when viewed, in white light, between crossed linear polarizer and analyser. Such a measuring system is capable of being automated and employed on a production line [1].

If the moulded polymer is opaque or translucent the photoelastic technique (employing transmitted light) cannot be used. When the moulding is in the form of a sheet then the residual stress can be evaluated by removing successive uniform layers of material from the surface of a test specimen and measuring the resulting curvature [2]. Similar observations can be made on sections of a complex moulding. In a variant of this method a small diameter hole is drilled in the test specimen and the relieved strain measured by surrounding strain gauges cemented on the polymer surface. The influence of frozen in strain on the long term stability of the moulding is demonstrated by accelerated ageing tests at elevated temperatures while the effects of surface stresses on stress corrosion is seen by immersing the test sample in the appropriate chemical solution.

The foregoing, time consuming, destructive tests, as applied to non-transparent polymer mouldings, cannot readily be used on the production line as a means of quality control, for which a simple non-destructive test is required. It was for this reason that a possible relationship between surface microhardness and processing conditions has been investigated for translucent polyethylene and transparent polystyrene. A future publication will compare these observations with photoelastic birefringence measurements.

2. Experimental procedure

Injection moulded plaques of overall dimensions $7.5 \times 7.5 \times 0.3\,cm^3$ were prepared from (i) high density polyethylene homopolymer Rigidex 07560 (BP Chemicals); (ii) high density polyethylene copolymer Rigidex 40M (BP Chemicals); (iii) homopolymer polystyrene, Carinex G.P (Shell Chemicals).

Rigidex 07560 was marketed as a narrow molecular weight distribution grade polymer characterized by high "toughness" and good processability, whereas Rigidex Type 40 is a broad molecular weight distribution injection moulding grade having good flow and moderate stress cracking resistance. The quoted values of density ϱ ($kg\,m^{-3}$) weight average molecular weights M_w and number average molecular weights M_n are (i) for Rigidex 07560, $\varrho = 964$, $M_w = 75000$, $M_n = 17000$; (ii) for Rigidex Type 40, $\varrho = 949$, $M_w = 95000$, $M_n = 9500$. The melt flow index (g per 10 min, 190° C), used as a measure of molecular weight, is given as 4 for Type 40 whereas that of 07560 is given as 8.

Carinex G.P. is marketed as a general purpose grade ideally suited for general injection moulding and in applications where fast cycling is required. The quoted value of ϱ is $1050–1070\,kg\,m^{-3}$.

2.1. Plaque manufacture

The plaques were produced on a Battenfeld BSKM 90/160 in line screw preplasticizing injection moulding machine. Molten polymer was injected through the

0022–2461/89 $03.00 + .12

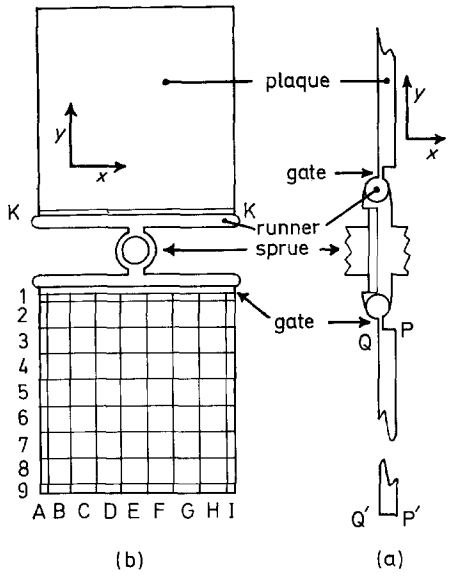

Figure 1 Side view (a) and plan view (b) of the pair of plaques obtained from the water cooled mould. During manufacture the position of the mould is such that the plane of the plaques is horizontal.

sprue into runners of 0.45 cm diameter. The polymer left each runner and entered the plaque mould through a gate having a rectangular cross-section of $7.5 \times 0.1\,cm^2$ and length 0.15 cm. The axis of the gate did not coincide with that of the plaque mould but was offset as shown in Fig. 1a. The water cooled mould produced a pair of plaques, as shown in Fig. 1b. One face of each plaque reproduced the highly polished mould surface whereas the opposing face carried an embossed reference grid, of 1 cm squares. Points on the plaque surface will be referred to this reference grid, labelled as in Fig. 1b.

The moulding parameters employed are listed in Table I. In this investigation of the influence of moulding parameters on plaque properties the front zone barrel temperature T_s and the mould temperature T_m were taken as the variables, but there were necessary associated changes in the other moulding parameters in order to preserve surface finish and to avoid the formation of flash, Table I.

Each moulding is identified by three numbers, the first being the value of T_s, the second the value of T_m and the third the shot number N in the sequence of plaques produced after an initial run to establish the operating conditions. The polyethylene Type 40M carries the further identification letter M.

All measurements were made on single plaques isolated from the complete moulding by cutting along line KK, Fig. 1, through that portion of the polymer which solidified in the gate.

2.2. Density measurements

Two holes, each of 1.3×10^{-2} cm diameter, were drilled near to opposing edges of each plaque so that a 10 g weight could be attached at one edge and the assembly (plaque plus weight) suspended from one arm of a microbalance. The assembly hung inside a container of deionized, deaerated water at 15° C. If W_h is the measured weight of the assembly when the water level covered the attached weight and W_H the measured weight when the water level covered weight plus plaque then the mean plaque density $\varrho = \varrho_w W_\varrho / (W_H W_h)$ where W_ϱ is the weight of the plaque alone. The density of water, ϱ_w, at 15° C is given as $999\,kg\,m^{-3}$ [3]. In the case of the polystyrene plaques the 10 g sinker weight was not required. Of the plaques produced at any given T_s, T_m density measurements were made on shot numbers $N = 1, 11, 21, 31, 41$.

2.3. Microhardness measurements

The microhardness V_H at points on each plaque surface was measured using the microhardness tester as

TABLE I

Moulding parameter	Rigidex Type 075–60 polyethylene						Rigidex Type 40M polyethylene						Carinex G.P. polystyrene		
Barrel temperature† (° C)															
hopper zone	150	240	150	240	150	240	150	240	150	240	150	240	150	180	210
middle zone	160	260	160	260	160	260	160	260	160	260	160	260	165	200	230
front zone	180	280	180	280	180	280	180	280	180	280	180	280	170	210	250
Melt temperature* (° C)	202	275	198	284	199	281	200	279	203	280	192	283	208	235	259
Mould temperature† (° C)	15	15	55	55	90	90	15	15	55	55	90	90	15	40	65
Cycle times* (sec)															
injection	18	24	21	37	24	48	15	22	19	33	22	46	11	13	19
cooling	12	16	15	14	19	12	12	15	15	15	17	12	14	15	38
screw back	7	7	7	7	6	7	7	6	6	6	7	7	11	11	12
total	39	47	45	60	50	68	39	45	45	57	50	69	34	39	67
Specific pressures* (MPa)															
injection	68	68	68	68	68	54	68	68	68	68	68	54	81	68	68
dwell	54	41	48	41	27	34	54	41	34	41	34	41	41	41	27
screw back	10	10	10	10	10	10	10	10	10	10	10	10	0	7	7
Clamp force* (kN)	580	710	580	710	580	710	580	710	580	710	580	710	420	420	420
Shot weight* (g)	40.2	39.3	39.0	39.1	37.5	38.1	39.2	38.5	37.8	38.1	37.2	37.4	44.2	44.7	43.8
Injection time* (sec)	0.8	0.7	3.1	3.1	2.6	3.6	0.8	0.7	1.1	0.9	2.5	2.7	0.75	1.3	2.2

†set values
*measured values

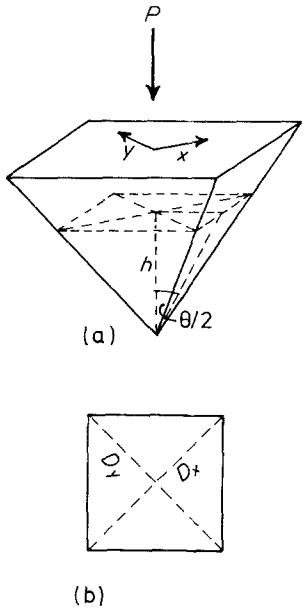

Figure 2 (a) The pyramidal diamond indenter used in the microhardness measurements. (b) Face diagonals D_x, D_y of the indentation.

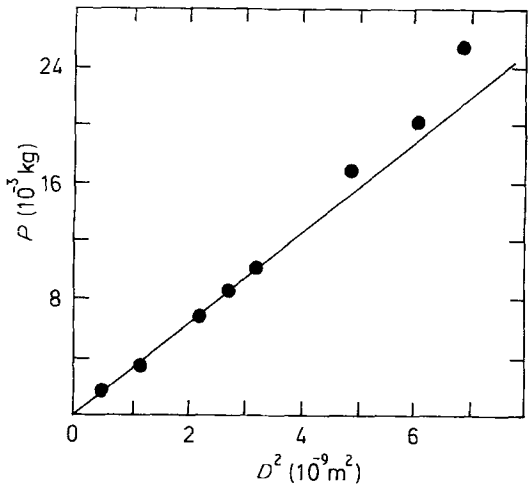

Figure 3 The variation of indentation parameter D(m) with load P (kg) applied for a time t of 6 sec. Measurements plotted as $P(10^{-3}\,\text{kg})$ against $D^2(10^{-9}\,\text{m}^2)$

fitted to the Reichert Universal optical microscope. With this instrument a spring loaded pyramidal shaped diamond indenter, having the form shown in Fig. 2a, is forced into the sample surface under an applied load P(kg) indicated on a scale visible in the microscope eyepiece. The load P was applied for t sec then the indenter was removed and the indentation face diagonals D_x, D_y measured using the micrometer and scale of the microscope eyepiece.

If, under the action of load P applied for t sec, the indenter sinks to a depth h, (Fig. 2a) then

$$h = \frac{D}{2\sqrt{2}} \frac{1}{\tan(\theta/2)} \tag{1}$$

and the face area A (m^2) of the indenter in contact with the solid is given by

$$A = \frac{D^2}{2\sin(\theta/2)} \tag{2}$$

where D(m) is the square face diagonal. The ratio P/A is a measure of the hardness of the solid and when, as here, $\theta = 136°$ then P/A gives the Vickers hardness number

$$V_H = \frac{P}{A} = \frac{2P}{D^2}\sin 68° = 18.192\frac{P}{D^2}\,(\text{Pa}) \tag{3}$$

The indenter sinks to a depth h such that the load P can be sustained by the polymer, the final deformation stage is probably elastic. The component of P perpendicular to the indenter face, $P_\perp = 0.93P$, imposes a compressive stress while the tangential component, $P_{||} = 0.375P$, imposes a shear stress. It follows that when the indenter is removed there is elastic recovery, the magnitude depending on the elastic moduli. Hence the final volume of the impression is less than that of the immersed indenter. This results in a decrease in impression parameter D although the effect may be masked by plastic deformation of the solid due to the larger imposed stresses at the indenter edges. Because of this elastic recovery factor Equation 2(3) is sometimes written as [4]

$$V_H = 18.192\frac{P}{(D + D_0)^2}\,(\text{Pa}) \tag{4}$$

where D and D_0 are the respective plastic and elastic contributions to the indentation parameter.

If the material is anisotropic then elastic recovery in one direction may be greater than that in the orthogonal direction. If, for example, elastic recovery only occurred parallel to the x direction, Fig. 2, then after removing the indenter it will be found that the indentation will no longer have a square cross section and that $D_x < D_y$ i.e. $V_{Hx} > V_{Hy}$. In the case of the moulded polymer plaque, it was anticipated that any anisotropy in V_H would be a maximum in the x, y directions indicated in Fig. 1. For this reason all the microhardness measurements were made with the indenter orientated such that the diagonals D lay in these directions, for every indentation D_x, D_y were measured.

Any systematic variation of V_H with indenter penetration depth h will lead to a continuous variation of measured V_H with load P; this will be seen as a non-linear dependence of D^2 on P. Fig. 3 shows the measured values of D^2 plotted against P for a series of indentations made within square E5, Fig. 1, of polyethylene sample 220/40/61. Measurements were made over the maximum range of P available, loading time $t = 6$ sec. Note that Equation 3 applies over the load range 0–10 g but that deviations occur at higher values of P. Consequently all measurements of V_H at any position on the plaque surface were made by making three closely spaced indentations at loads P of 3.3, 6.7 and 10 g weight and taking the mean value of P/D^2.

Scanning electron microscope (SEM) pictures of microhardness indentations in polyethylene and polystyrene are given in Section 3.3.

In all measurements of microhardness the time t (sec) for which the load P is applied can have an important bearing on measured V_H. With hard (i.e. large V_H) materials the indenter rapidly attains its equilibrium position and there is no observed change in impression parameter D (and hence measured V_H)

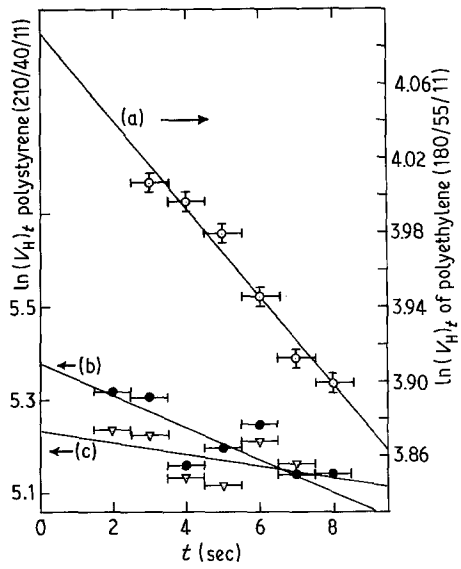

Figure 4 The measured values of V_H plotted against the time, t for which the load P was applied to the indenter. Measurements were made at square E5 on (a) polyethylene 180/55/11, for P = 6.6 g (b) polystyrene 210/40/11, for P = 6.6 g (c) polystyrene 210/40/11, for P = 10 g.

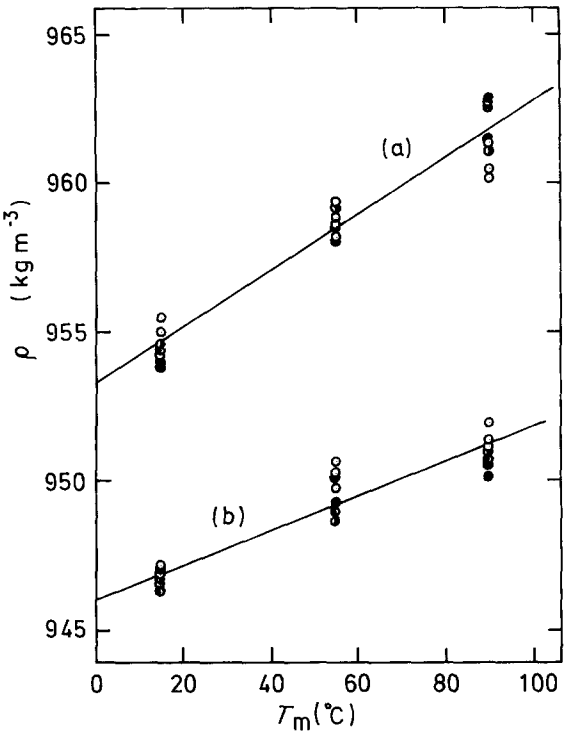

Figure 5 The mean density ϱ of each polyethylene plaque plotted against its mould temperature T_m. (a) polyethylene Type 075 60 (b) polyethylene Type 40M. The front zone barrel temperature T_s employed for each plaque is denoted by ● T_s = 280° C, ○ T_s = 180° C.

with loading time t. For soft materials however D is an increasing function of t which can be expressed as

$$(V_H)_t = (V_H)_0 t^{-\alpha} \quad (5)$$

where α is a load dependent "creep parameter". These features are illustrated in Fig. 4 which shows the V_H against t dependence at square E5 on (a) polyethylene 180/55/11 and (b) polystyrene 210/40/11. Each value of V_H was the average value of four indentations produced under a load P = 6.6 g applied for a specific time t in the range 2–8 sec.

The polyethylene measurements are well described (correlation 0.98) by Equation 5 with $(V_H)_0$ = 59.51 MPa and $\alpha = 2.36 \times 10^{-2}$ (c.f. $\alpha = 5 \times 10^{-2}$ in ultra orientated polyethylene [4]) whereas the harder polystyrene is approximately described (correlation 0.84) by $(V_H)_0$ = 216 MPa and $\alpha = 3.4 \times 10^{-2}$. Also shown in Fig. 4 is the $(V_H)_t$ against t graph, (c), for polystyrene when P = 10 g, now the value of $\alpha = 1 \times 10^{-2}$ but strongly affected by experimental scatter.

In all subsequent measurements of V_H, as determined from the graphs of P against D^2, the load P was applied for a time t = 5 sec.

2.4. Microscopic examination

Reflection scanning electron microscope (SEM) pictures have been taken of the microhardness indentations formed on the moulded polyethylene and polystyrene (xy) plaque surfaces.

Prior to SEM examination all the samples were sputter coated with a thin film of gold.

3. Experimental results

3.1. Visual appearance of plaques

The design of the mould was such that plaques of different thickness could be produced by altering the position of plate PP′ with respect to plate QQ′, Fig. 1a. Polyethylene plaques 0.1 cm thick showed two-dimensional curvature due to residual strain, the centre of curvature being to the left of QQ′. The 0.3 cm thick polyethylene and polystyrene plaques used in this investigation were not visibly distorted.

Visually the 075 60 and Type 40M polyethylene plaques appeared identical. Both types were opalescent and on nearly all the plaque surfaces flow marks were evident in the vicinity of of the moulding gate. Away from the gate area the plaques retained the highly polished surface of the mould, one face of each plaque also carried the reference grid described in Fig. 1. The "glass clear" polystyrene plaques did not show flow marks.

3.2. The average plaque density

3.2.1. Polyethylene

The measured mean density ϱ (kg m^{-3}) of each 075 60 plaque and of each Type 40M plaque is shown plotted against its mould temperature T_m (°C) in Fig 5, the experimental points also identify the value of T_s. A linear regression analysis of the experimental points of Fig. 5 gave

$$\varrho = (9.55 \times 10^{-2})T_m + 953.3 \quad (6)$$

correlation 0.97, for 075 60 and

$$\varrho = (5.812 \times 10^{-2})T_m + 946.0 \quad (7)$$

correlation 0.95, for Type 40M.

There was no correlation between ϱ and T_s.

3.2.2. Polystyrene

The measured ϱ values are shown plotted in Fig. 6 against T_m and also against $T_s - T_m$. The mean value of ϱ for each set of plaques (indicated by x) lies very

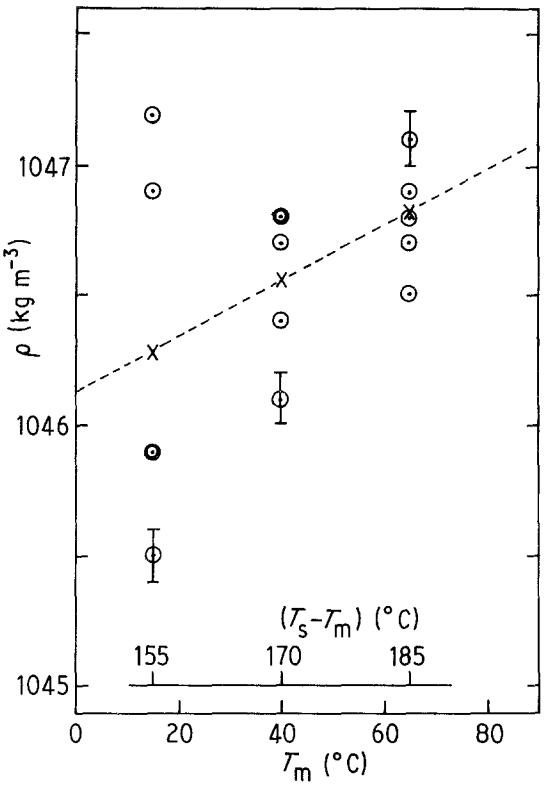

Figure 6 The mean density ϱ of each polystyrene plaque plotted against its mould temperature T_m and also against $(T_s - T_m)$. The symbol x denotes the average value of ϱ for each set of plaques produced at given T_m.

close to a straight line represented by

$$\varrho = (1.06 \times 10^{-2})T_m + 1046.14 \quad (8a)$$

or

$$\varrho = (1.77 \times 10^{-2})(T_s - T_m) + 1043.5 \quad (8b)$$

but it is notable that the spread in ϱ values of plaques manufactured at any T_m decreases as T_m increases.

Earlier measurements on the effect of cooling rate and applied pressure [5, 6] on the density of polystyrene have shown that if the polystyrene is raised to a temperature 30° C above the glass temperature T_g (where $T_g = 105°C$ at 1 atmosphere and $\partial T_g/\partial P = 0.03°C\,bar^{-1} = 0.3°C\,MPa^{-1}$) then the density ϱ *decreases* with increasing solidification cooling rate r, i.e. $\partial\varrho/\partial r$ is negative but $|\partial\varrho/\partial r|$ is independent of pressure P. Similarly the pressure dependence of the density, $\partial\varrho/\partial P$, is positive and non-zero for $P < 207$ MPa but independent of r.

At the injection pressures used in manufacturing the plaques namely 81 or 68 MPa the values of T_g are 130 or 125.4° C. Thus in every case the temperature T_s of the polystyrene is at least 40° C greater than T_g (for the appropriate definition of T_g see [7]). The injection pressure variation between samples is such to give negligible effect on the density, the only remaining parameter is thus the cooling rate r. If r is proportional to $(T_g - T_m)$ say rather than $(T_s - T_m)$ then the measurements given in Fig. 6 are consistent with the published isobaric results but obviously influenced by the rheological nature of the injection process.

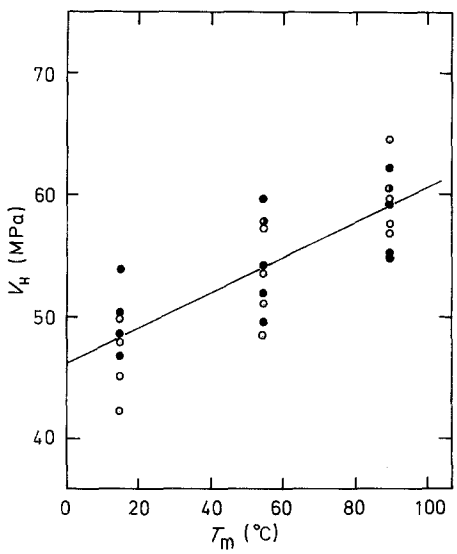

Figure 7 The measured value of V_H (MPa) for each polyethylene plaque. Type 075 60, plotted against its mould temperature T_m (°C). The front zone barrel temperature T_c employed for each plaque is denoted by ● $T_s = 280°C$, ○ $T_s = 180°C$.

3.3. Microhardness

3.3.1. Polyethylene

In all the plaques examined there was, for any given plaque, no significant variation in V_H over the surface of the plaque neither was there any evidence of hardness anisotropy since it was always found that $D_x = D_y$. Similarly it has been reported [8] that the typical injection moulding grade Lupolen 6011L ($M_w = 100\,000$) shows an approximately linear dependence of ϱ on T_m but no hardness anisotropy whereas the very high molecular weight grade Lupolen 5261 Z ($M_w = 450\,000$) did show the hardness anisotropy also exhibited by ultradrawn polyethylene [4].

The measured values of V_H for the 075 60 and Type 40M plaques are shown plotted as graphs of V_H against T_m in Figs 7 and 8 respectively. The best straight line through the experimental points is given by

$$V_H = 0.144T_m + 46.025 \quad (9a)$$

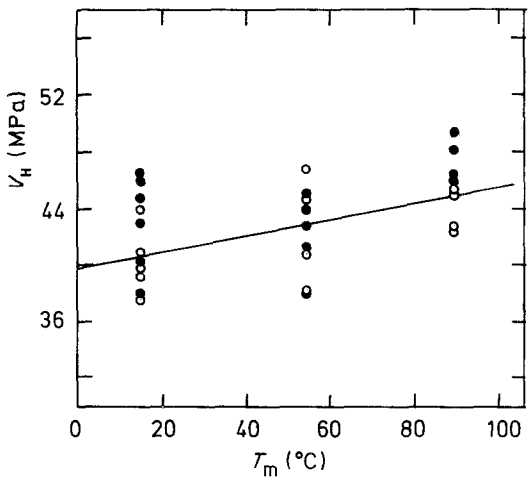

Figure 8 The measured value of V_H (MPa) for each polyethylene plaque. Type 40M, plotted against its mould temperature T_m (°C). The front zone barrel temperature T_s employed for each plaque is denoted by ● $T_s = 280°C$, ○ $T_s = 180°C$.

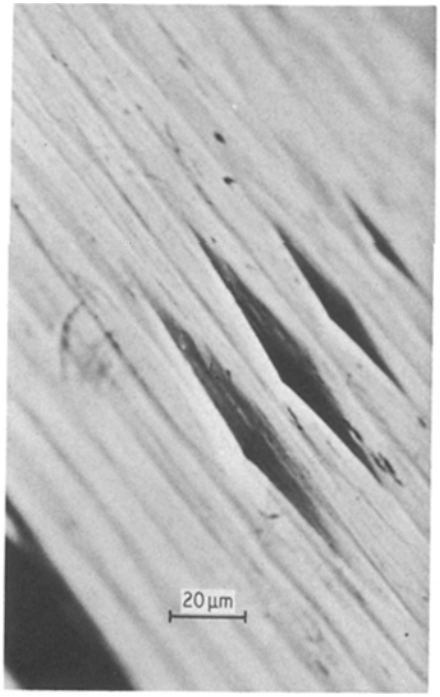

Figure 9 A SEM oblique angle view of a row (parallel to the x axis) of four indentations produced on square H8 of polyethylene sample 220/40/11. The indentations were produced under loads of 58.3, 41.7, 24.0 and 8.3 g respectively, the largest indentation being in the foreground.

Figure 10 A higher magnification view of the largest indentation of Fig. 9 showing part of the indentation perimeter.

for the 075 60 plaques and

$$V_H = 0.056T_m + 39.907 \quad (9b)$$

for the Type 40M plaques.

In the microhardness measurements V_H was determined from the face diagonals D of indentations produced at loads of 3.3, 6.7 and 10 g weight. Fig. 9 shows a SEM oblique angle view of a row (parallel to the x axis) of four indentations produced on square H8 of a sample 220/40/11. The indentations were produced under loads of 58.3, 41.7, 25.0 and 8.3 g respectively, the largest indentation being in the foreground of Fig. 9. The face diagonal D of this largest indentation, as measured from Fig. 9, is 1.08×10^{-2} cm giving a $V_H = 91$ MPa. This value of V_H is very much greater than any shown in Fig. 7 and is another illustration of how V_H increases with load P at the larger values of P, Fig. 3.

It follows from Equation 1 that the largest indentation of Fig. 9 has a depth $h = 15\,\mu$m and an indentation volume $V = (4h^3 \tan^2 68°)/3 = 2.76 \times 10^{-9}$ cm^3. If the displaced material had been transported to the surface to form a raised lip around the perimeter ($2\sqrt{2}D = 3.05 \times 10^{-2}$ cm) of the impression then the height d and lateral extent L of the lip would be given by $dL = 0.9 \times 10^{-6}$ cm^2. For any likely combination of d and L this raised lip should be evident in Fig. 9 and even more so in Fig. 10 which shows part of the largest indentation perimeter at higher magnification. The absence of any discernable lip together with the general appearance of the indentation leads to the conclusion that no plastic flow occurred and the indentation formed as a result of compaction of underlying material.

On the basis that V_H gives a measure of the local density of the solid, i.e. the less dense the material the more it has to be compressed to reach a value at which it can support the applied load P, so a V_H against plaque density relationship should emerge from Figs 5, 7 and 8. This is shown in Fig. 11 where the measured V_H value for each polyethylene plaque is plotted against its mean density ϱ. A least squares straight line fit to all the measurements given in Fig. 11, i.e. for Type 075 60 and Type 40M, is given by

$$V_H = 1.169\varrho - 1067 \quad (10)$$

correlation 0.87. Also shown in Fig. 11 are the published, graphical values of V_H, ϱ for Lupolen 6011 L [8] and these exhibit similar behaviour.

3.3.2. Polystyrene

In Fig. 12a the measured V_H values for the 170/15/N plaques are plotted against the position at which they were measured i.e. at the centres of reference squares E2, E5, E8 and B8. The numbers shown against each point indicate the shot number N of the plaque concerned. Considering position E2, located 1 cm from the mould gate, it is seen that the spread in measured V_H at this position between the different plaques extends from $V_H = 159$ MPa to 202 MPa but there is no systematic variation with N. At position E5 (the plaque centre) the spread in V_H extends from 183 to 215 MPa, again there is no systematic variation with N. At positions E8 and B8 the spread in V_H is from 157 to 233 MPa and from 185 to 204 MPa respectively.

Figs 12b and c show measured V_H at the different positions for plaques moulded at $T_m = 40$ and 65° C. As in Fig. 12a the spread in V_H is least at the centre position E5 but the spread in V_H values at the other positions E2, E8, B8 reduces as T_m increases.

Since position E5 showed the least sample variation

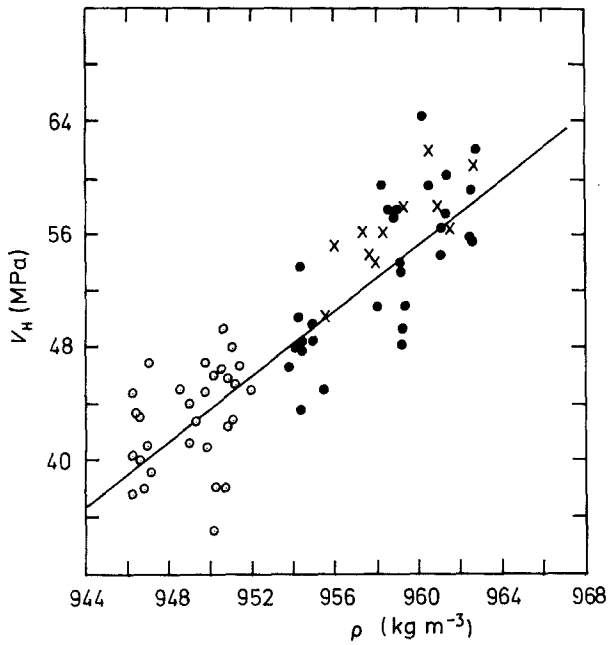

Figure 11 The measured microhardness V_H (MPa) of Type 075 60 (●) and Type 40M (○) polyethylene plaques plotted against plaque density ϱ. Also shown (X) are the V_H, ϱ values for injection moulded Lupolen 6011L polyethylene bars [8].

at any T_m these E5 values of V_H were plotted against T_m. This graph (not given here) showed there was no change in V_H at E5 as the T_m changed from 40° C to 65° C; the scatter in V_H at T_m = 15° C made the graph uncertain over the range 15 to 40° C.

To summarize the V_H measurements on polystyrene it would seem that (a) the mean V_H is independent of T_m (b) variations in V_H occur at the gate and plaque extremities (and are, therefore, likely to be a rheological feature) the variations diminishing as T_m increases.

Fig. 13 shows a normal incidence SEM view of three microhardness indentations produced in polystyrene under loads P of 6.66, 10 and 33.32 g respectively. The 10 g indentation is the largest that was used in the V_H measurements. Note that the largest (33.32 g) indentation has compression rings in its vicinity. These "rings" are even more evident in Fig. 14 which shows indentations produced under loads of 166.6 g and 83.3 g respectively.

When viewed obliquely, Fig. 15, the "rings" surrounding the largest indentation are seen to be ripples produced on the plaque surface by the strain field of the indentation.

The depth h of the 166.6 g indentation, Figs 14 and 15, as calculated from measured D and Equation 1, is 18.6 μm, which is comparable with that of the polyethylene indentation shown in Fig. 9. It has been shown [9] that indentations of this depth in polystyrene can be completely removed by annealing at temperatures around 100° C. The rate of recovery $(\partial h/\partial t)$ is initially rapid but the later part of the recovery is described by second-order kinetics (activation energy 163 kcal mol^{-1}) attributed to a mechanism involving the motion and annihilation of defects of opposite sign. Comparing Figs 9 and 10 with Figs 14 and 15 it would appear that the indentation mechanism in polystyrene is different to that of the softer polyethylene.

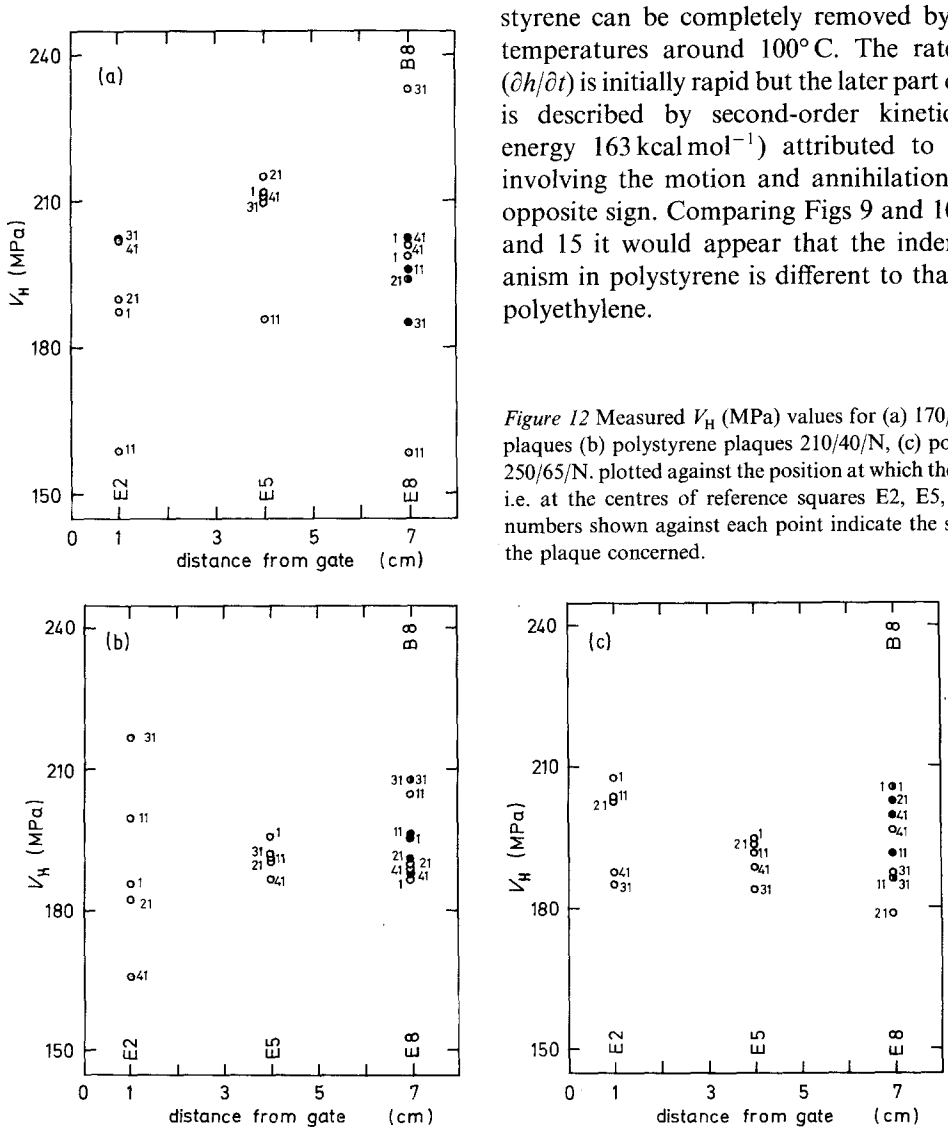

Figure 12 Measured V_H (MPa) values for (a) 170/15/N polystyrene plaques (b) polystyrene plaques 210/40/N, (c) polystyrene plaques 250/65/N. plotted against the position at which they were measured, i.e. at the centres of reference squares E2, E5, E8, B8 (●). The numbers shown against each point indicate the shot number N of the plaque concerned.

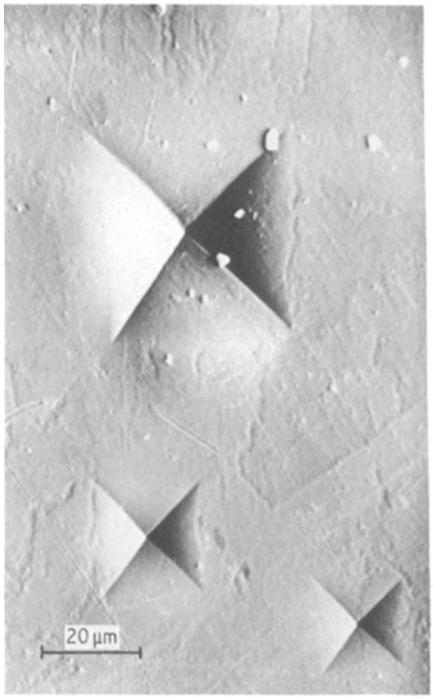

Figure 13 A normal incidence SEM view of three microhardness indentations produced in polystyrene under loads P of 6.66, 10 and 33.32 g respectively.

Figure 14 A normal incidence SEM view of two microhardness indentations produced in polystyrene under loads P of 83.3 and 166.6 g respectively.

In the case of polystyrene, where there is only a small variation of mean density ϱ with T_m, Equation 8, the scatter is measured V_H due to variations in V_H across the plaque surface effectively masks any V_H, ϱ dependence.

4. Discussion

During the formation of the polymer plaque liquid polymer enters the mould via the gate, Fig. 1, so that a liquid flow front advances between the walls PP′, QQ′ of the mould. The mechanism of mould filling by a developing front has been the subject of detailed mathematical analysis based on hydrodynamic lubrication theory [10–19]. Liquid polymer coming into contact with the mould walls, at temperature T_m, solidifies so that viewed perpendicular to the narrow cross sections PP′QQ′ there is a solidified layer growing out from the walls and an approximately isothermal hot core through which the melt flows in a Poiseuille type shearing motion. At the flow front the melt from the central region flows outwards like a fountain to the mould walls where it solidifies. After the mould is filled the melt becomes stationary and cools and vitrifies under the action of the applied pressure.

As far as molecular orientation within the plaque is concerned it is thought that near the mould walls the orientation, or lack of it, is that associated with the fountain flow at the liquid front. Moving away from the wall the molecular orientation will be that associated with the stream line flow of the melt as it passed between the vitrified layers in contact with the walls. The thickness of these vitrified layers at the end of the ing where the melt vitrified under quasi static conditions there may be no net molecular orientation.

Polyethylene and polystyrene both possess the same hydrocarbon backbone chain so that the molecular orientation accompanying mould filling is expected to be similar for both polymers. However polyethylene is a crystallizable polymer (exhibiting mass fraction crystallinities in the range 20–80%) whereas atactic polystyrene is not. Microscopic examination of the polyethylene plaque cross-section shows a fibrous crystalline structure, associated with oriented molecules, which persists through the thickness of the plaque to within approximately 5 μm of the xy plaque surface [20]. The disordered state of the xy surface molecules is that of the boundary layer set down by the fountain flow front. Pictorial evidence of the molecular orientation produced during mould filling is also shown by the birefringence patterns seen in polystyrene plaques [20].

4.1. The density and microhardness of polyethylene

The homopolymer Rigidex 075 60 and the copolymer Rigidex 40M both showed a systematic increase in mean plaque density ϱ (i.e. percentage crystallinity) with mould temperature T_m with $(\partial\varrho/\partial T_m)$ for Type 075 60 (M_w = 85 000) approximately twice that for the broad molecular weight distribution polymer Type 40M (M_w = 95 000), Fig. 5. The increase in ϱ with T_m is evidently associated with the decreased cooling rate.

In the microhardness measurements, 3.3.1, the range of P employed was such that the depth h of the

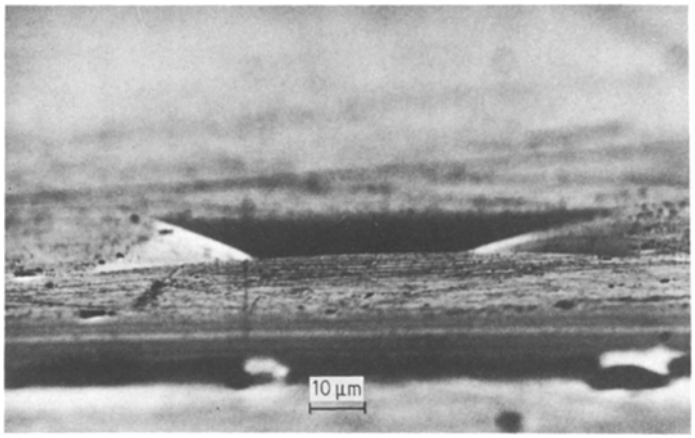

Figure 15 An oblique angle SEM view of a microhardness indentation in polystyrene produced under load P' of 166.6 g.

predominantly that of the comparatively disordered surface layers and for this reason there was no evidence of hardness anisotropy. With increasing load P there was an increase in measured V_H, Fig. 3, which, provided the indentation mechanism is unchanged, is due to the increased hardness of the underlying oriented polymer. Nonetheless for both polymers there is a good correlation between the surface V_H and mean density ϱ over the complete range of moulding conditions, Equation 10, Fig. 11. The influence of this skin core morphology on the mechanical properties of injection mouldings has been investigated [21–27].

Since there were no detectable variations in V_H over the xy surface of each polyethylene plaque, it would seem that the local density variations are quite small. In the case of more complicated mouldings, where local variations in T_m are possible, it is possible that V_H may give a good indication of the local density (i.e. percentage crystallinity) in the moulding.

4.2. Density and microhardness of polystyrene

As described in section 3.2.2 the variation in polystyrene plaque density with T_s, T_m, Fig. 6, is consistent with isobaric measurements only if the polymer cooling rate is proportional to $(T_g - T_m)$ rather than $(T_s - T_m)$. The value of $(\delta\varrho/\partial T_m)$ is smaller than in polyethylene and increasing T_m substantially reduces the scatter in ϱ values.

In the microhardness measurements, section 3.2.2, there was no evidence of the hardness anisotropy which might have occurred if any oriented molecular layer had extended sufficiently close to the plaque surface to influence the visible face diagonals of the indentation, Fig. 13. The spread in V_H values observed, at any one position, in a batch of plaques produced at given T_m diminishes as T_m increases, Fig. 12. At higher values of T_m the plaques are evidently less sensitive to the inevitable small fluctuations in manufacturing parameters and this results in a more consistent mould filling and cooling cycle. This also accounts for the reduction in the spread of ϱ values.

5. Conclusions

Within the range of injection moulding parameters T_s, T_m employed the following general conclusions as to the influence of these parameters on V_H and ϱ of the moulded plaques.

5.1. Polystyrene

Increasing T_m reduces the variation in V_H (but not the mean) over the plaque surface and gives a small but systematic increase in mean plaque density ϱ, Equation 8, with an associated decrease in the spread of ϱ vealues.

5.2. Polyethylene

As in polystyrene the V_H measurements indicate that the moulded plaques contain a molecularly disordered thin surface layer. However the indentation mechanism in polyethylene is different from that in polystyrene. Changing the moulding parameters revealed a linear dependence of ϱ on T_m, Equations 6 and 7 attributed to changes in percentage crystallinity. There is also a linear dependence of V_H on T_m and these relations combine to give the common linear V_H plotted against ϱ dependence. Equation 10, of Type 07560 and 40M (also Lupollen 6011 L). The surface microhardness V_H can thus be used as a measure of the local density (percentage crystallinity).

The actual measurement of V_H is sufficiently straightforward that it could form the basis of a method of quality control.

Acknowledgements

The author gratefully acknowledges the advice and cooperation of J. Roberts and R. A. Tickner of RARDE. The work described here was done under

References

1. A. REDNER, *Plast. Eng.* Feb. (1987) 37.
2. R. G. TREUTING and W. T. READ Jr, *J. Appl. Phys.* **22** (1951) 130.
3. "American Institute of Physics Handbook" (McGraw Hill Book Co., New York, 1972).
4. F. J. BALTA CALLEJA, D. R. RUEDA, R. S. PORTER and W. T. MEAD, *J. Mater. Sci.* **15** (1980) 765.
5. A. ZEHAVI and F. E. FILISKO, *J. Macromol. Sci. Phys.* **B21** (1982) 47.
6. R. F. ROE, *J. Appl. Phys.* **48** (1977) 4085.
7. I. G. BROWN, R. E. WETTON, M. J. RICHARDSON and N. G. SAVILL, *Polymer* **19** (1978) 659.
8. D. R. RUEDA, F. J. BALTA CALLEJA and R. K. BAYER, *J. Mater. Sci.* **16** (1981) 3371.
9. B. T. A. CHANG and J. C. M. LI, *J. Mater. Sci.* **15** (1980) 1364.
10. R. L. BALLMAN, T. SHUSMAN and H. L. TOOR, *Mod. Plast.* **37** (1959) 105.
11. I. M. BARRIE, *Plast. Polym.* **37** (1969) 463.
12. M. R. KAMAL and S. KENIG, *Polym. Engng Sci.* **12** (1972) 294.

13. J. L. BERGER and C. G. GOGOS, *ibid.* **13** (1973) 209.
14. J. L. WHITE, *ibid.* **15** (1975) 44.
15. M. R. KAMAL, Y. KUO and P. H. DOAN, *ibid.* **15** (1975) 863.
16. E. BROYES, C. GUTFINGER and Z. TADMOR, *Trans. Soc. Rheol.* **19** (1975) 423.
17. J. F. STEVEN, A. GALSKY, K. K. WANG, I. CHEN and D. H. REBER, *Polym. Engng Sci.* **17** (1977) 666.
18. J. L. WHITE and W. DIETZ, *ibid.* **19** (1979) 1081.
19. A. I. ISAYEV and C. A. HIEBER, *Rheol. Acta.* **19** (1980) 168.
20. B. L. EVANS, To be published.
21. E. S. CLARK, *Plast. Eng.* **30** (1974) 73.
22. M. R. KANTZ, H. D. NEWMAN and F. H. STIGALE, *J. Appl. Polym. Sci.* **16** (1972) 1249.
23. V. TAN and M. R. KAMAL, *ibid.* **22** (1978) 2341.
24. M. FUJIYAMA, H. AWAYA and S. KIMURA, *ibid.* **21** (1977) 3291.
25. M. FUJIYAMA and S. KIMURA, *ibid.* **22** (1978) 1225.
26. M. FUJIYAMA and K. AZUMA, *ibid.* **23** (1979) 2807.
27. S. Y. HOBBS and C. F. PRATT, *ibid.* **19** (1975) 1701.

Received 9 December 1987
and accepted 11 March 1988